

Modeling some drying characteristics of sour cherry (*Prunus cerasus* L.) under infrared radiation using mathematical models and artificial neural networks

R. Amiri Chayjan¹, M. Kaveh², S. Khayati¹

(1. Department of Biosystems Engineering, Faculty of Agriculture, Bu-Ali Sina University, 6517833131, Hamedan, Iran;

2. Young researchers club, Sardasht Branch, Islamic Azad University, Sardasht, Iran)

Abstract: The effect of air temperature, air velocity and infrared (IR) radiation on the drying kinetics of sour cherry was investigated using a laboratory infrared dryer. Experiments were conducted at air temperatures of 35, 50 and 65°C, air velocities of 0.5, 1.1 and 1.7 m/s and IR radiations of 500, 1,000 and 1,500 W. Five empirical drying models for describing time dependence of the moisture ratio change were fitted to experimental data. Artificial neural network (ANN) method was used to predict the effective moisture diffusivity and specific energy consumption of the samples. Among the applied models, Midilli et al. model was the best to predict the thin layer drying behavior of sour cherry. Effective moisture diffusivity of sour cherry varied between 1.17×10^{-10} and 8.13×10^{-10} m²/s. Activation energy of sour cherry was in the range of 30.31–41.68 kJ/mol. Specific energy consumption was in the range of 56.12–891.16 MJ/kg. After well training of the ANN models, it proved that the ANN model was relatively better than the empirical models. The best neural network feed and cascade forward back-propagation topologies for the prediction of effective moisture diffusivity and energy consumption were the 3-2-3-1 and 3-3-3-1 structures with the training algorithm of trainlm and threshold functions of tansig, tansig-logsig-tansig, respectively. The best R^2 value for predication of moisture diffusivity and energy consumption were 0.9944 and 0.9905, respectively.

Keywords: sour cherry, drying, effective moisture diffusivity, activation energy, artificial neural network

Citation: R. Amiri Chayjan, M. Kaveh, and S. Khayati. 2014. Modeling some drying characteristics of sour cherry (*Prunus cerasus* L.) under infrared radiation using mathematical models and artificial neural networks. Agric Eng Int: CIGR Journal, 16(1): 265–279.

1 Introduction

The sour cherry (*Prunus cerasus* L.) is mainly produced in Poland, U.S.A., Turkey, Russian Federation, Serbia, Hungary, Iran, Austria, Azerbaijan and Germany. Based on food and agriculture organization statistics, Iran produced about 102,574 t of sour cherry in 2011, which was approximately 5% of the world's sour cherry production (FAO, 2011). Sour cherry is used to prepare different products such as beverages, sauces, jelly, candy, pastilles and jam (Aghbashlo et al., 2010). The main

goal in agricultural and food products drying is the reduction of their moisture content to a specific level, allowing safe storage over an extended period of time. For a longer storage life, product diversity and a substantial volume reduction, fruits and vegetables drying is popular (Basman and Yalcin, 2011). Thin layer drying models are used to predict drying time for food and agricultural products and also to generalize the kinetics of drying process. Drying kinetics of foodstuffs is greatly affected by air velocity, air temperature and material characteristics (Erenturk and Erenturk, 2007).

One of the most popular drying methods of food and agricultural materials with high moisture content is infrared radiation. Infrared (IR) heating is an efficient

Received date: 2013-05-30 Accepted date: 2013-12-25

Corresponding author: R. Amiri Chayjan, Email: amirireza@basu.ac.ir.

food processing technology and has gained a great interest in food industry due to its advantages over conventional heating. Certain characteristics like thermal efficiency, fast heating rate/response time, wavelength, direct heat penetration into the product and reflectivity make IR heating more effective for some applications and provide considerable reduction in energy consumption (Sakai and Mao, 2006). Infrared heating has applications in drying, baking, roasting, blanching, pasteurization and sterilization of food products. It has been applied to reduce moisture content of various agricultural products including grains, legumes, fruit and vegetables (Khir et al., 2011; Nimmol et al., 2007).

Some physical and thermal properties of food and agricultural products, such as moisture diffusion, heat and mass transfer, specific energy and activation energy consumption are important for a proper dryer design (Aghbashlo et al., 2008). Some researchers have studied activation energy and moisture diffusion in a thin layer drying of various agricultural and food products. These include rough rice (Khir et al., 2011), carrot (Togrul, 2006), paddy (Das et al., 2009), soybean (Niamnuy et al., 2012) and grape (Ruiz Celma et al., 2009a).

In order to correlate effective parameters with complex relationships, artificial neural network (ANN) can be used as a popular method. ANN has been demonstrated in patterning complex relationships between input and output data and has been applied successfully in many food processing applications (Shafafi Zenoozian and Devahastin, 2009). Most of the studies on drying using neural networks are based on Multilayer Perceptron (MLP) neural networks with back propagation learning algorithm. These methods have been used to expose the effects of the drying conditions such as air temperature, moisture, and flow rate on the drying process (Cakmak and Yildiz, 2011). An important benefit of ANNs over statistical methods is that they require no assumptions about the form of a model. Instead, the ANN is trained with experimental data to find a suitable topology; so it is becoming a very popular estimating approach and is known to be less time-consuming and efficient in modeling of complex systems compared to mathematical and statistical models

(Pahlavan et al., 2012). Many studies have been conducted on application of ANNs in drying of food and agriculture products (Menlik et al., 2010; Mohebbi et al., 2011; Motevali et al., 2013).

Although, many information has been gathered about the activation energy and effective moisture diffusivity for various agricultural and food products, any published literature is not available on the activation energy and effective moisture diffusivity for sour cherry during infrared drying and modeling with artificial neural networks. The main objectives of this research were to determine the activation energy, effective moisture diffusivity and specific energy consumption of sour cherry during infrared thin layer drying process and model it with input air temperature, air velocity and IR radiation. Also, the aim of this research is to develop and evaluate the feed and cascade forward artificial neural networks topology as an approximate tool for prediction of moisture diffusivity and energy consumption performance of infrared radiation drying process.

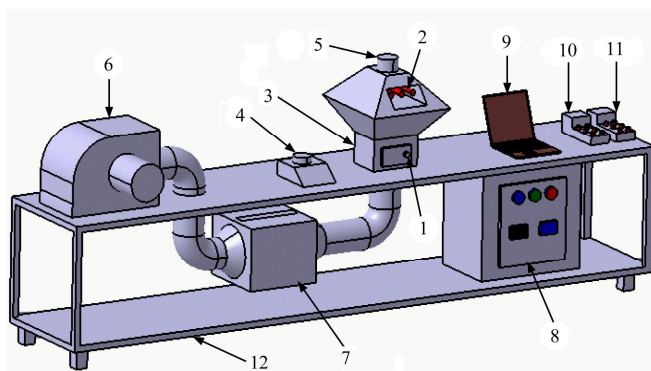
2 Materials and methods

2.1 Drying conditions

Freshly harvested sour cherries were purchased from a market in Hamedan, Iran and stored in the refrigerator at about $4\pm 1^{\circ}\text{C}$ for experiments. Generally, samples of uniform sizes were selected. The immature and spoiled sour cherries were separated manually. The initial moisture content of sour cherry was determined by oven method. About 30 g of the sample was dried in an oven at $70\pm 1^{\circ}\text{C}$ for about 24 h (ASAE, 2007). At least five replicates of experiment were made.

A laboratory infrared dryer was developed at the Biosystems Engineering Department of Bu-Ali Sina, University, Hamedan, Iran for this study (Figure 1). The essential parts of dryer system consists of an adjustable centrifugal blower, four infrared lamps (Philips, Belgium) with 2,000 W power, electrical air heating chamber (2.4 kW), drying chamber, inverter (LS, Korea) and thermostat (Atbin, Iran) and a tray sample. Mean values of environmental parameters such as ambient air temperature and air relative humidity ranged between 29

to 35°C and 22% to 28%, respectively. Accuracy of thermometer (Lutron TM-903, Taiwan) with sensor type k was 0.5% reading+1°C and accuracy for humidity meter (Lutron TM-903, Taiwan) for relative humidity lower than 70% was ±3% RH and for upper than 70% was ± 3% reading + 1% RH. During the experiments, the ambient air temperature, air relative humidity and inlet and outlet temperatures of the dryer chamber were recorded. After 30 min when the dryer conditions reached the steady state, the dryer was loaded by 30±1 g sour cherries and drying process started. Experiments were performed at 35, 50 and 65°C. At each temperature, three velocity values and three lamp IR radiations were adjusted: 0.5, 1.1 and 1.7 m/s also 500, 1,000 and 1,500 W, respectively. Samples were weighed during the drying process using a digital balance with 0.01 g accuracy. Drying process was carried out using samples with initial moisture content of about 2.05 (d.b.) and terminated when the moisture content decreased to about 0.19 (d.b.).



1. Drying chamber 2. Lamp infrared 3. Air temperature sensor 4. Precision balances 5. Air velocity sensor 6. Fan and electrical motor 7. Electrical heater 8. Inverter and thermostat 9. Computer 10. Thermometer 11. Psychrometer 12. Chassis

Figure 1 Schematic diagram of laboratory scale infrared dryer

Before the start of any experiment, the dryer system was started in order to achieve a desirable steady-state condition. Experiments were replicated three times. In this study, the influence of the drying conditions on the effective moisture diffusivity, activation energy and specific energy consumption in thin-layer drying of sour cherry are explained.

2.2 Theoretical principal

Moisture content was calculated using the following equation:

$$M = \frac{((W_0 - W) - W_1)}{W_1} \tag{1}$$

where, M is the moisture content, $g_{\text{water}}/g_{\text{dry matter}}$; W_0 is the initial weight of sample, g; W is the amount of evaporated moisture, g; and W_1 is the dry matter content of sample, g (Shen et al., 2011).

The moisture content values obtained for the drying temperatures of 35, 50 and 65°C were converted into the moisture ratio (MR). The dimensionless moisture ratio might be obtained using the following equation (Ponkham et al., 2011):

$$MR = \frac{(M_t - M_e)}{(M_0 - M_e)} \tag{2}$$

The moisture ratio was simplified to M_t/M_0 , where M_t and M_0 are the moisture content at any given time and the initial moisture content, respectively.

During drying of sour cherry in the infrared dryer, M_e values were relatively small compared to M_t and M_0 . So Equation (2) was simplified as follow (Khir et al., 2011):

$$MR = \frac{M_t}{M_0} \tag{3}$$

Fick’s second law of diffusion with spherical coordinates was applied in this study. The assumptions in Fick’s equation solution were: moisture migration in diffusion, negligible volume shrinkage, constant temperature and diffusion coefficients (Crank, 1975):

$$MR = \frac{M_t - M_e}{M_0 - M_e} = \frac{6}{\pi^2} \sum_{n=1}^{\infty} \frac{1}{n^2} \exp\left(\frac{-D_{eff} n^2 \pi^2 t}{r^2}\right) \tag{4}$$

where, MR is the moisture ratio, decimal; M_t is the moisture content at any time, $kg_{\text{water}}/kg_{\text{dry matter}}$; M_e is the equilibrium moisture content, $kg_{\text{water}}/kg_{\text{dry matter}}$; M_0 is the initial moisture content, $kg_{\text{water}}/kg_{\text{dry matter}}$; $n = 1, 2, 3...$ is the number of terms taken into consideration; t is the drying time, s; D_{eff} is the effective moisture diffusivity, m^2/s ; and r is the radius of kernel, m.

For longer drying periods, Equation (4) can be simplified to first term of series only, without much affecting the accuracy of the prediction (Odjo et al., 2012):

$$\ln(MR) = \ln\left(\frac{M_t - M_e}{M_0 - M_e}\right) = \ln\left(\frac{6}{\pi^2}\right) - \left(\frac{D_{eff} \pi^2 t}{r^2}\right) \tag{5}$$

Then:

$$MR = \left(\frac{6}{\pi^2}\right) \exp\left(-\frac{\pi^2 D_{eff} t}{r^2}\right) \tag{6}$$

The slope (K_1) is calculated by plotting $\ln(MR)$ versus time according to Equation (5) (Aghbashlo et al., 2008):

$$K_1 = \left(\frac{D_{eff} \pi^2}{r^2}\right) \tag{7}$$

The temperature dependency of the effective moisture diffusivity is represented by a well-known Arrhenius-type correlation:

$$D_{eff} = D_0 \exp\left(\frac{E_a}{R_g T_a}\right) \tag{8}$$

For determining E_a , Equation (8) can be written as follow:

$$\ln(D_{eff}) = \ln(D_0) - \left(\frac{E_a}{R_g} \cdot \frac{1}{T_a}\right) \tag{9}$$

where, D_0 is the pre-exponential factor, m^2/s ; E_a is the activation energy of diffusion, J/mol ; T_a is the absolute air temperature, K ; and R_g is the universal gas constant, $8.314 J/(mol K)$.

The determination of coefficient (R^2) was one of the primary criteria for selecting the best equation to define a suitable model. In addition to R^2 , the various statistical parameters such as reduced chi-square (χ^2) and root mean square error ($RMSE$) were used to determine the quality of the fit. These parameters can be calculated as follows:

$$R^2 = 1 - \frac{\sum_{i=1}^N [MR_{exp,i} - MR_{pre,i}]^2}{\left[\sum_{k=1}^N \frac{\sum_{i=1}^N MR_{pre,i}}{N} - MR_{pre,i} \right]^2} \tag{10}$$

$$\chi^2 = \frac{\sum_{i=1}^N (MR_{exp,i} - MR_{pre,i})^2}{N - z} \tag{11}$$

$$RMSE = \left[\frac{1}{N} \sum_{i=1}^N (MR_{pre,i} - MR_{exp,i})^2 \right]^{\frac{1}{2}} \tag{12}$$

where, $MR_{exp,i}$ stands for the experimental values and $MR_{pre,i}$ for predicted values by calculating from the model for this measurements. N and z are the number of observations and constants, respectively.

Equation (5) can also be written in a more simplified form as follow:

$$MR = \frac{M - M_e}{M_b - M_e} = \exp(-kt^n) \tag{13}$$

Equation (13) is known as a single exponential equation. The empirical models were used as alternative approaches to analyze thin layer drying. Some commonly used equations in thin layer drying studies are shown in Table 1. In order to select a suitable model describing the drying process of sour cherry with high moisture content, drying curves were fitted with thin layer drying equations.

2.3 Specific energy consumption

Specific energy consumption (SEC) for sour cherry drying was obtained using the following equation (Amiri Chayjan et al., 2011):

$$SEC = (C_{pa} + C_{pv} h_a) Q t \frac{(T_{in} - T_{am})}{m_v V_h} \tag{14}$$

where, C_{Pv} and C_{Pa} are specific heat capacity of vapor and air, respectively, 1004.16 and $1828.8 J kg^{-1} °C^{-1}$; Q is the inlet air to drying chamber, m^3/s ; t is the total drying time, min ; h_a is absolute air humidity, $kg_{vapor}/kg_{dry air}$; T_{in} and T_{am} are inlet air to drying chamber and ambient air temperatures, respectively, $°C$; m_v is mass of removal water, kg ; and V_h is specific air volume, m^3/kg .

Table 1 Thin layer drying models used in modeling of sour cherry

Model	Equation	Reference
Demir et al.	$MR = a \exp(-kt^n) + b$	Demir et al. (2007)
Midilli et al.	$MR = a \exp(-kt^n) + bt$	Midilli et al. (2002)
Wang and Singh	$MR = 1 + ax + bx^2$	Motevali et al. (2013)
Logestic	$MR = a / (1 + b \exp(kt))$	Cihan et al. (2007)
Logarithmic	$MR = a \exp(-kt) + c$	Ruiz Celma et al. (2012)

Note: a, b, c, k and n are constants.

2.4 Artificial neural network

Feed and cascade forward neural networks are the most common types of artificial neural networks (ANN). These networks used for prediction of outputs of new unknown patterns. Furthermore, in this research, feed and cascade forward networks as well as several learning algorithms were utilized. Feed forward back propagation (FFBP) consists of one input layer, one or several hidden layers and one output layer (Demuth et al.,

2007). For learning this network, back propagation (BP) learning algorithm was used. In the case of BP algorithm, the first output layer weights were updated. The weight coefficient was updated by weight values and learning rules. During training this network, calculations were carried out from input of network toward output and values of error were then propagated to prior layers. Cascade forward back propagation (CFBP) is similar to FFBP network in using the BP algorithm for weights updating, but the main symptom of this network is that, each layer neurons relates to all previous layer neurons. Two training algorithms including Levenberg-Marquardt (LM) and Bayesian regulation (BR) back propagation algorithms were used for updating network weights.

Applying the three inputs in all experiments, the effective moisture diffusivity and specific energy consumption values derived for different conditions. Networks with three neurons in input layer (air velocity, air temperature and IR radiation) and one neuron in output layer (D_{eff} and SEC) were designed.

Figure 2 shows the considered neural network topology and input and output parameters. Boundaries and levels of input parameters are shown in Table 2. Neural network toolbox of Matlab software (The MathWorks Inc., Natick, Massachusetts, USA) was used in this study.

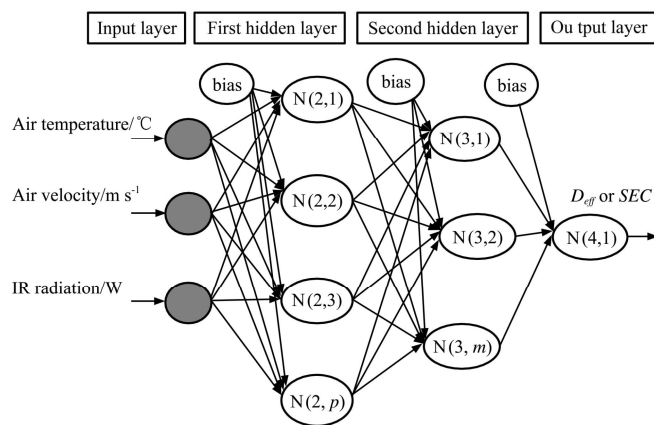


Figure 2 Artificial neural network topology for modeling effective moisture diffusivity or energy consumption of sour cherry fruit

The increasing method was used for selection layers and neurons for evaluation of various topologies. By this method, when the network was trapped into the local

minimum, new neurons were gradually added to the network.

Table 2 Input parameters for artificial neural networks and their boundaries for prediction of effective moisture diffusivity, specific energy consumption of sour cherry

Parameters	Minimum	Maximum	No. of levels
Air temperature/°C	35	65	3
Air velocity/m s ⁻¹	0.5	1.7	3
IR radiation/W	500	1500	3

Various threshold functions were used to reach the optimized status (Demuth et al., 2007):

$$Y_j = X_j \quad (\text{PURELIN}) \quad (15)$$

$$Y_j = \frac{2}{(1 + \exp(-2X_j)) - 1} \quad (\text{TANSIG}) \quad (16)$$

$$Y_j = \frac{1}{1 + \exp(-X_j)} \quad (\text{LOGSIG}) \quad (17)$$

where, X_j is the sum of weighed inputs for each neuron in j^{th} layer and computed as below:

$$X_j = \sum_{i=1}^m W_{ij} \times Y_i + b_j \quad (18)$$

where, m is the number of output layer neurons; W_{ij} is the weight of between i^{th} and j^{th} layers; Y_i is i^{th} neuron output and b_j is bias of j^{th} neuron for FFBP and CFBP networks. Experimental data of 35, 50 and 65°C were selected for training network with suitable topology and training algorithm. About 75% of all data were randomly selected for training network with suitable topology and training algorithm.

To optimize the selected network from prior stage, the secondary criteria were R^2 , $RMSE$ and the following equations:

$$MAE = \frac{100}{n} \sum_{k=1}^n \left| \frac{S_k - T_k}{T_k} \right| \quad (19)$$

$$SD_{MAE} = \sum_{k=1}^n \sqrt{\frac{(S_k - T_k)^2}{df}} \quad (20)$$

where, R^2 is the determination coefficient; MAE is the mean absolute error; SD_{MAE} the standard error; S_k is the network output for k^{th} pattern; T_k is the target output for k^{th} pattern; df is the degree of freedom and n is the number of training patterns. To increase the accuracy and processing velocity of network, input data were

normalized at boundary of (0, 1).

3 Results and discussion

3.1 Drying kinetic

Changes in the moisture content with time during the drying process of sour cherry are shown in Figure 3. The moisture content decreased continuously with time. At three different temperatures (35, 50 and 65°C) and IR radiation (500, 1,000 and 1,500 W) such values for the time period were determined as 1,150, 850, 700, 540, 460, 390, 310, 270, and 240 min, 1,050, 860, 670, 570, 480, 400, 330, 280 and 230 min and 1,110, 880, 670, 530, 450,

380, 300, 240 and 210 min at an airflow rate of 0.9, 1.76 and 2.6 m/s, respectively (final moisture content 0.19 d.b.). According to the results, drying air temperature and IR radiation have an important role in drying. High drying temperatures induce rapid decrease of sour cherry moisture content. When the air temperature and IR radiation was increased, the drying time was reduced. This phenomenon is because of applying more energy rate to the bed material and increasing in drying rate. The results are similar to the earlier studies of drying paddy (Das et al., 2009) and soybean grains (Dondé et al., 2011).

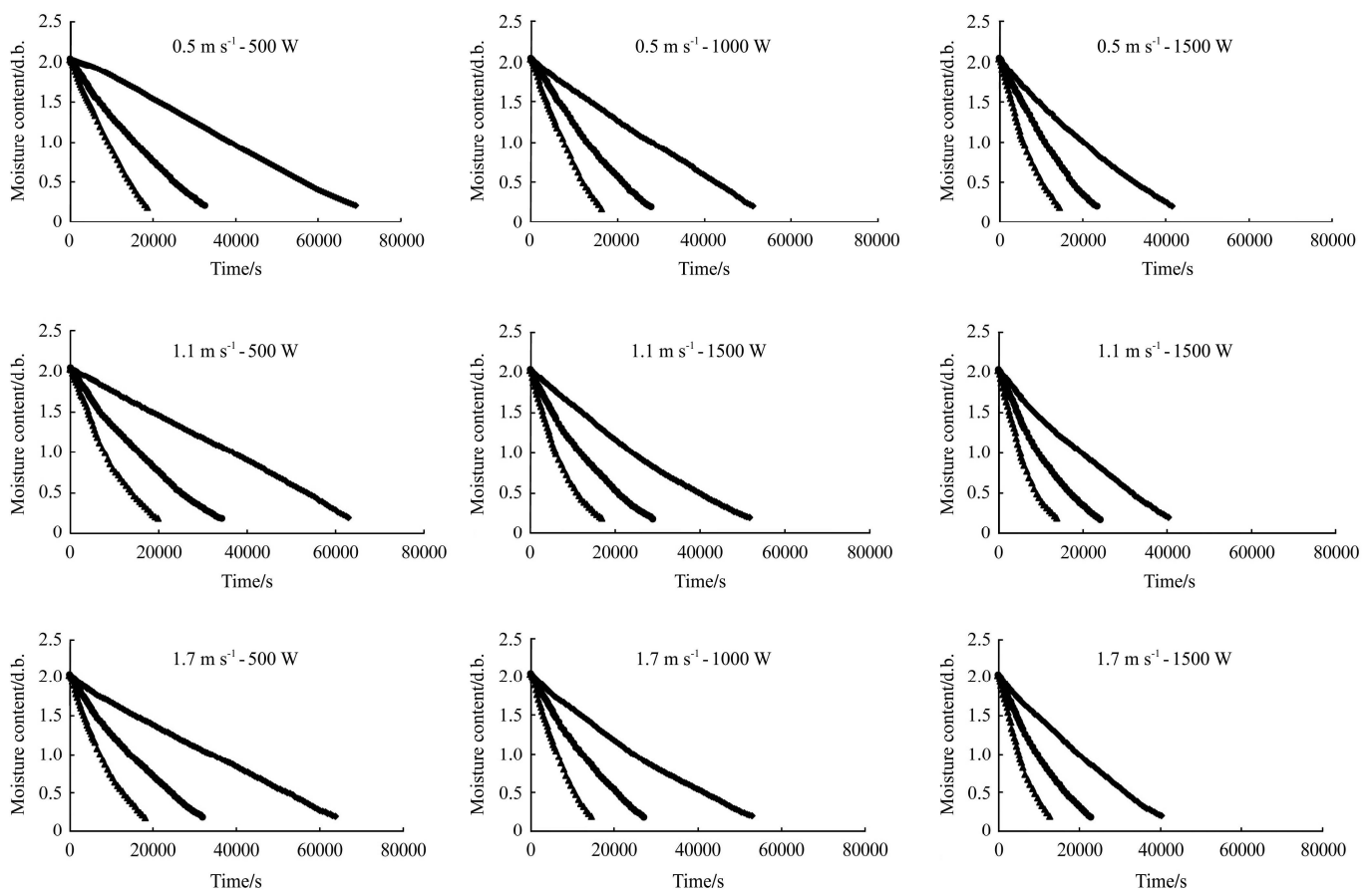


Figure 3 Moisture content of sour cherry fruit at different IR radiations, drying air temperatures (\blacklozenge 35°C, \bullet 50°C and \blacktriangle 65°C) and air velocities

Drying curves (Figure 3) and obtained curves after plotting $\ln(MR)$ against time in Figure 4 and drying rate in Figure 5, proved that all drying cases of sour cherry were happened in falling rate period. Similar results have been observed in drying some agricultural products such as tomato (Ruiz Celma et al., 2009b), castor oil seeds (Perea-Flores et al., 2012) and squash seed (Amiri

Chayjan et al., 2013b).

The effects of drying temperature, air velocity and IR radiation on drying rate of the sour cherry are given in Figure 5. Drying rate showed an increase at the beginning of the process due to sample heating. After an initial short period the drying rate reached a maximum value and then it followed falling rate in all drying

conditions. No constant drying rate period was observed. Similar results were reported by previous researchers (Markowski et al., 2010; Thuwapanichayanan et al., 2011; Zielinska and Cenkowski, 2012). Drying rate at the initial of the process was affected by air velocity, especially at the temperature of 65°C, which implies that evaporation initially took place at the surface and being therefore more directly affected by air velocity. The initial surface evaporation was gradually replaced by an evaporation front that receded to the interior of the solid. The predominance of air velocity was therefore succeeded by the moisture diffusion process, which became the most important factor (Yadollahinia and Jahangiri, 2009).

The model coefficients for all the four models were estimated by non-linear regression technique using commercial software of Curve Expert 3. A regression analysis was conducted for these empirical models by

relating the drying time and dimensionless moisture ratio at each drying temperature. Goodness of fit of the models is characterized by the highest value of coefficient of determination (R^2) and lowest values of root mean square error ($RMSE$) as well as reduced Chi-square (χ^2). The statistical results of the different models, including the comparison criteria used to evaluate goodness of fit, viz., the values of coefficient of determination (R^2), root mean square error ($RMSE$) and reduced Chi-square (χ^2) are presented in Table 3. It was found that the Midilli et al. model shows best fit to the experimental drying data with lower $RMSE=0.0362$ and $\chi^2=0.0019$ and higher $R^2=0.9994$ as compared to the other models. Therefore the Midilli et al. model was selected to describe the drying behavior of high moisture sour cherry under infrared radiation. Table 4 presents the estimated values of parameters in Midilli et al. model depending on IR radiation, air velocity and drying air temperature.

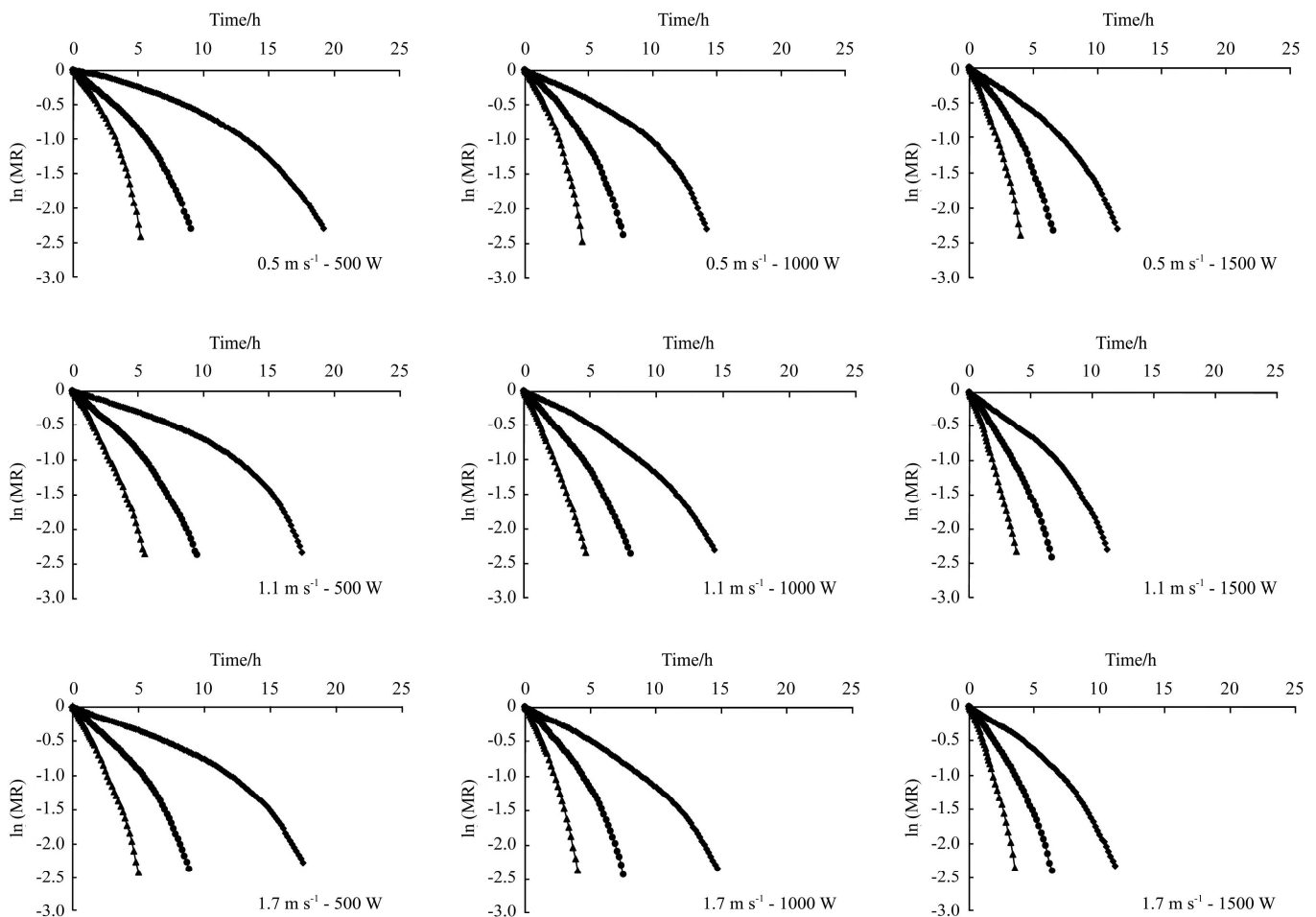


Figure 4 Ln(MR) versus time (hour) for different air velocities, IR radiations and drying air temperatures (◆ 35°C, ● 50°C and ▲ 65°C)

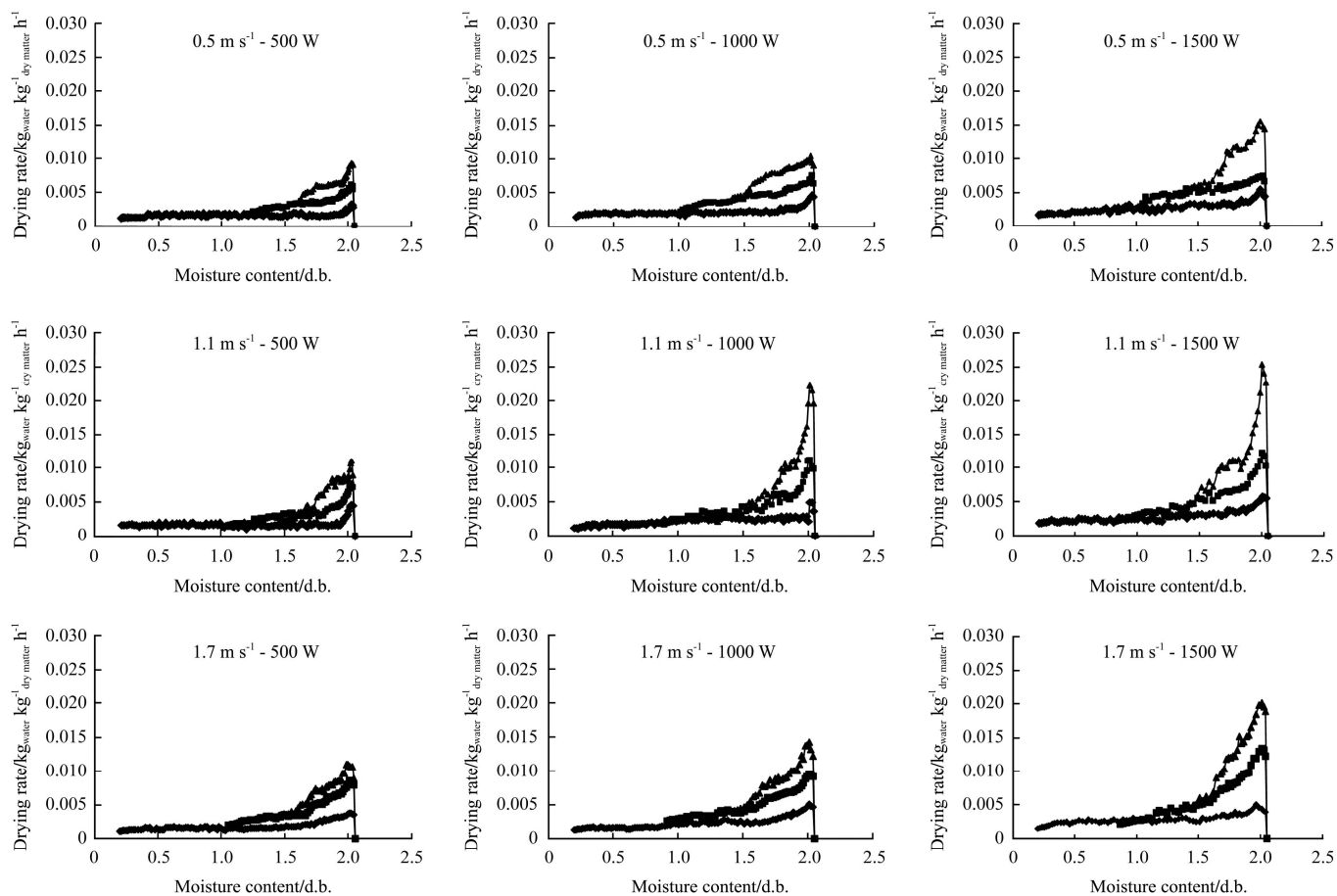


Figure 5 Relationship between drying rate and moisture content of sour cherry at different IR radiations, drying air temperatures (◆ 35°C, ■ 50°C and ▲ 65°C) and air velocities

Table 3 The statistical comparison for prediction of thin layer drying of sour cherry fruit

Model	Temperature/°C- IR radiation/W	R^2			χ^2			RMSE		
		0.5 m/s	1.1 m/s	1.7 m/s	0.5 m/s	1.1 m/s	1.7 m/s	0.5 m/s	1.1 m/s	1.7 m/s
Demir et al.	35-500	0.9975	0.9991	0.9994	0.0170	0.0049	0.0035	0.1289	0.0234	0.0693
	50-500	0.9996	0.9993	0.9995	0.0014	0.0023	0.0015	0.0362	0.0183	0.0462
	65-500	0.9996	0.9973	0.9995	0.0007	0.0059	0.0008	0.0261	0.0161	0.0729
	35-1000	0.9997	0.9996	0.9996	0.0011	0.0021	0.0018	0.0319	0.0142	0.0450
	50-1000	0.9996	0.9995	0.9987	0.0011	0.0013	0.0006	0.0323	0.0089	0.0349
	65-1000	0.9997	0.9990	0.9998	0.0004	0.0018	0.0002	0.0195	0.0324	0.0398
	35-1500	0.9995	0.9990	0.9995	0.0021	0.0041	0.0018	0.0441	0.0382	0.0624
	50-1500	0.9998	0.9994	0.9996	0.0003	0.0015	0.0007	0.0184	0.0267	0.0374
65-1500	0.9985	0.9979	0.9975	0.0027	0.0034	0.0039	0.0486	0.0409	0.0548	
Midilli et al.	35-500	0.9998	0.9997	0.9998	0.0013	0.0023	0.0007	0.0364	0.0365	0.0259
	50-500	0.9998	0.9996	0.9970	0.0005	0.0011	0.0098	0.0220	0.0313	0.0954
	65-500	0.9997	0.9988	0.9997	0.0005	0.0027	0.0006	0.0220	0.0494	0.0237
	35-1000	0.9997	0.9998	0.9969	0.0013	0.0009	0.0151	0.0359	0.0304	0.1221
	50-1000	0.9998	0.9997	0.9997	0.0005	0.0008	0.0005	0.0217	0.0280	0.0225
	65-1000	0.9998	0.9993	0.9998	0.0003	0.0013	0.0003	0.0172	0.0344	0.0172
	35-1500	0.9990	0.9995	0.9997	0.0004	0.0017	0.0011	0.0621	0.0409	0.0310
	50-1500	0.9998	0.9996	0.9998	0.0003	0.0007	0.0003	0.0183	0.0267	0.0167
65-1500	0.9993	0.9985	0.9993	0.0012	0.0024	0.0011	0.0323	0.0464	0.0315	

Model	Temperature/°C- IR radiation/W	R^2			χ^2			RMSE		
		0.5 m/s	1.1 m/s	1.7 m/s	0.5 m/s	1.1 m/s	1.7 m/s	0.5 m/s	1.1 m/s	1.7 m/s
Wang and Singh	35-500	0.9989	0.9994	0.9981	0.0077	0.0032	0.0101	0.0870	0.0565	0.1050
	50-500	0.9992	0.9984	0.9985	0.0028	0.0056	0.0048	0.0526	0.0738	0.0685
	65-500	0.9995	0.9980	0.9998	0.0011	0.0045	0.0003	0.0320	0.0659	0.0192
	35-1000	0.9996	0.9997	0.9994	0.0031	0.0015	0.0031	0.0556	0.0392	0.0553
	50-1000	0.9987	0.9982	0.9996	0.0012	0.0052	0.0011	0.0317	0.0708	0.0336
	65-1000	0.9987	0.9990	0.9996	0.0005	0.0018	0.0007	0.0229	0.0411	0.0257
	35-1500	0.9988	0.9982	0.9989	0.0051	0.0074	0.0044	0.0708	0.0851	0.0660
	50-1500	0.9998	0.9994	0.9996	0.0004	0.0014	0.0008	0.0214	0.0367	0.0282
65-1500	0.9999	0.9983	0.9983	0.0019	0.0028	0.0029	0.0426	0.0512	0.0524	
Logestic	35-500	0.9992	0.9973	0.9973	0.0054	0.0161	0.0161	0.0726	0.1253	0.1247
	50-500	0.9981	0.9979	0.9985	0.0066	0.0071	0.0049	0.0794	0.0824	0.0688
	65-500	0.9982	0.9986	0.9997	0.0039	0.0032	0.0005	0.0603	0.0548	0.0204
	35-1000	0.9980	0.9997	0.9993	0.0099	0.0013	0.0032	0.0981	0.0360	0.0560
	50-1000	0.9996	0.9990	0.9993	0.0011	0.0029	0.0019	0.0323	0.0528	0.0436
	65-1000	0.9984	0.9994	0.9992	0.0029	0.0011	0.0014	0.0527	0.0316	0.0363
	35-1500	0.9983	0.9974	0.9981	0.0071	0.0102	0.0077	0.0829	0.1008	0.0858
	50-1500	0.9988	0.9996	0.9997	0.0031	0.0012	0.0007	0.0540	0.0317	0.0266
65-1500	0.9993	0.9989	0.9993	0.0011	0.0017	0.0011	0.0326	0.0391	0.0324	
Logarithmic	35-500	0.9973	0.9989	0.9994	0.0181	0.0066	0.0035	0.1350	0.0805	0.0589
	50-500	0.9981	0.9993	0.9995	0.0066	0.0023	0.0016	0.0794	0.0467	0.0393
	65-500	0.9996	0.9974	0.9996	0.0007	0.0059	0.0008	0.0265	0.0744	0.0283
	35-1000	0.9997	0.9996	0.9996	0.0011	0.0021	0.0013	0.0322	0.0453	0.0430
	50-1000	0.9996	0.9996	0.9997	0.0011	0.0013	0.0006	0.0327	0.0353	0.0241
	65-1000	0.9997	0.9990	0.9998	0.0004	0.0018	0.0003	0.0198	0.0405	0.0182
	35-1500	0.9995	0.9990	0.9995	0.0020	0.0041	0.0019	0.0444	0.0628	0.0438
	50-1500	0.9998	0.9994	0.9997	0.0003	0.0015	0.0007	0.0188	0.0379	0.0272
65-1500	0.9997	0.9979	0.9997	0.0027	0.0034	0.0039	0.0495	0.0559	0.0600	

Table 4 Coefficients of Midilli et al. model for prediction of kinetic drying of sour cherry fruit

Air velocity /m s ⁻¹	Coefficients	35°C-500 W	50°C-500 W	65°C-500 W	35°C-1000 W	50°C-1000 W	65°C-1000 W	35°C-1500 W	50°C-1500 W	65°C-1500 W
0.5	a	1.381	1.010	1.009	0.669	0.994	1.000	0.526	1.000	0.987
	k	0.303	0.112	0.122	-0.376	0.128	0.197	-0.594	0.134	0.393
	n	-0.039	0.840	0.830	-0.026	1.140	0.934	-0.035	0.976	1.201
	b	-0.051	-0.046	-0.110	-0.059	-0.023	-0.089	-0.073	-0.059	-0.232
1.1	a	0.939	1.000	0.981	0.987	0.998	0.983	1.021	0.982	0.976
	k	-0.052	0.121	0.277	0.061	0.186	0.379	0.103	0.225	0.424
	n	-0.044	0.825	1.251	1.161	0.931	1.110	0.724	1.139	1.191
	b	-0.004	-0.043	0.006	-0.010	-0.024	-0.005	-0.041	-0.003	-0.012
1.7	a	0.656	0.488	0.998	0.523	0.992	1.01	1.012	0.984	0.981
	k	-0.387	-0.636	0.307	-0.596	0.154	0.319	0.064	0.211	0.459
	n	0.045	-0.053	1.091	-0.043	1.041	1.039	0.634	1.120	1.269
	b	-0.046	-0.093	-0.014	-0.582	-0.024	-0.047	-0.062	-0.013	0.004

3.2 Effective moisture diffusivity

The effective moisture diffusivity of foodstuffs characterizes its intrinsic mass transport property of moisture which includes molecular diffusion, liquid

diffusion, vapor diffusion, hydrodynamic flow and other mechanisms (Ruiz Celma et al., 2009b). The average effective moisture diffusivity (D_{eff}) was calculated by taking the arithmetic mean of the effective moisture

diffusivities that were estimated using Equations (6) and (7) at various levels of moisture content during the course of the drying. The values of D_{eff} for all drying conditions are presented in Figure 6. The D_{eff} of high moisture sour cherry was found to vary between the 1.18×10^{-10} to 8.13×10^{-10} m²/s. The effective diffusion coefficient for foodstuff is mostly between 10^{-12} to 10^{-9} m²/s (Aghbashlo et al., 2008). The average effective moisture diffusivity was found to increase with increase in IR radiation intensity at any particular velocity. This may be because, the increase in radiation intensity caused rapid rise in temperature of the product, which in turn increased the vapor pressure and consequently led to faster drying diffusion of moisture towards the surface (Shi et al., 2008). Also D_{eff} increased with increasing air temperature for any particular radiation intensity level. Similar results have been observed in drying some agricultural products such as apple slices (Zhu et al., 2010), rough rice (Khair et al., 2011) and soybean (Niamnuy et al., 2012).

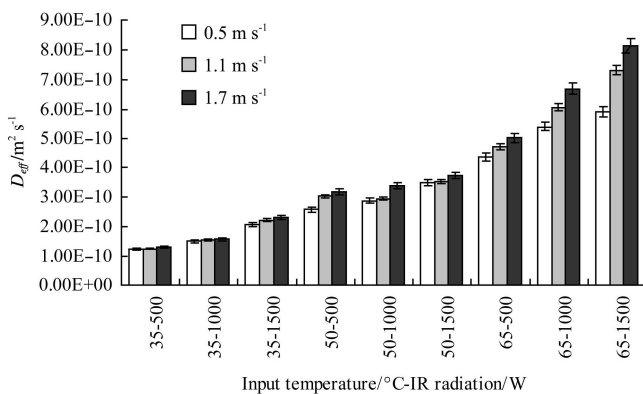


Figure 6 D_{eff} versus air temperature (°C) and IR radiation (W) for drying of sour cherry fruit

The relationship between D_{eff} and the independent variables is as follow:

$$D_{eff} = 3.08 \times 10^{-11} + 3.08 \times 10^{-11} v + 7.04 \times 10^{-11} P + 2.09 \times 10^{-10} T_c + 3.26 \times 10^{-11} v T_c + 3.49 \times 10^{-11} P T_c + 5.95 T_c^2$$

$$R^2 = 0.9752 \quad (21)$$

where, v is the air velocity, m/s; T_c is the air temperature, °C; and P is the IR radiation, W.

3.3 Activation energy

For determining activation energy, at first, $1/T_a$ values were plotted against $\ln(D_{eff})$ as shown in Figure 7. Then

activation energy (E_a) was calculated using Equation (12). E_a values for different air velocity levels, temperatures and IR radiations and related R^2 values are presented in Table 5. Values of E_a for food and agricultural products generally varied between 12 to 130 kJ/mol. The calculated minimum and maximum values of E_a for sour cherry were 30.31 and 41.68 kJ/mol, respectively. Two water form in food products are free and bounded moisture. Most of the water in sour cherry fruit is in the form of free moisture. But the surface skin of the fruit prevents the remove of moisture. As a result, the sample drying was accomplished in falling rate period. This phenomenon causes a relatively increase in activation

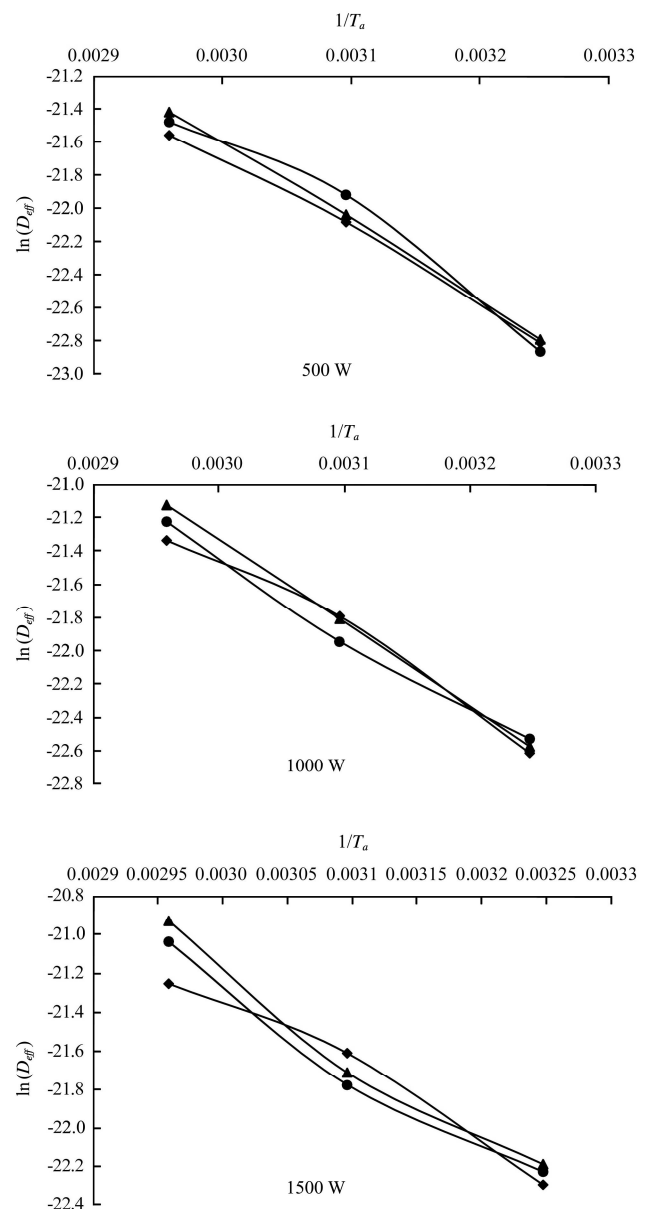


Figure 7 $\ln(D_{eff})$ against $1/T_a$ at different bed conditions (♦ 0.5 m/s, ● 1.1 m/s and ▲ 1.7 m/s) for thin-layer drying of sour cherry fruit

energy of sour cherry. In this period, air velocity and temperature have no significant effect on moisture transfer. So increase in drying air velocity causes increase in energy consumption. Increases in drying air temperature tend to damages in physical and chemical characteristics. If appropriate levels of IR radiation, air velocity and temperature applied for sour cherry drying, damages should be decreased (Aghbashlo et al., 2008). Maximum value of E_a was obtained at air velocity of 1.7 m/s and IR radiation of 1,000 W. This value for

sour cherry using a laboratory scale static-type dryer was determined as 64.39 to 66.05 kJ/mol by Aghbashlo et al. (2010). A higher E_a value indicated a greater temperature sensitivity of diffusion coefficient. It can be seen that the diffusion coefficient for 1.7 m/s was the most sensitive temperature. The average value of this parameter for blueberries was obtained as 66.3 kJ/mol (Shi et al., 2008). The average value of this parameter for grape was calculated as 19.27 kJ/mol (Ruiz Celma et al., 2009a).

Table 5 Activation energy values and related correlation coefficient for different bed conditions in drying periods of sour cherry fruit

Air velocity/m s ⁻¹ - Infrared/W	0.5- 500	0.5- 1000	0.5- 1500	1.1- 500	1.1- 1000	1.1- 1500	1.7- 500	1.7- 1000	1.7- 1500
Activation energy/kJ mol ⁻¹	36.24	36.99	30.31	40.14	37.49	34.15	39.81	41.68	36.09
Coefficient of determination (R^2)	0.9954	0.981	0.9760	0.9675	0.9925	0.9744	0.9991	0.9999	0.9738

3.4 Specific energy consumption

During the experiments, the specific energy consumption (SEC) for removing 1 kg moisture content from sour cherry by the use of an infrared convective dryer was calculated for each experiment using Equation (14). Computed values of SEC is shown in Figure 8. It was observed that the SEC decreased as drying air temperature decreased. Increasing air velocity affected intensively increase in SEC . Maximum value of SEC (891.1 MJ/kg) obtained at air velocity of 1.7 m/s with drying air temperature of 65°C and IR radiation of 500 W. The minimum value of SEC calculated 56.1 MJ/kg while air velocity, drying air temperatures and IR radiation were 0.5 m/s, 35°C and 1,500 W, respectively. Increasing in IR radiation caused decrease in SEC values. Also increasing in air velocity led to an intensive increase in SEC value. Results emphasized that applying of lower IR radiation and higher air velocity caused an intensive increase in energy consumption compared to the other conditions. Accordingly, low IR radiation level with low air velocity caused a relative decrease in moisture diffusivity, leading to higher SEC values. With the increase in IR radiation and slow down air velocity, the drying time is reduced. By reducing the drying time, specific energy consumption is reduced. Results proved that increasing in drying time affected on SEC inversely. In other words, each factor caused an increase in drying

time, also caused an increase in energy consumption for each temperature. Similar results have been obtained for paddy (Khoshtaghaza et al., 2007), berberis fruit (Aghbashlo et al., 2008), and terebinth seed (Amiri Chayjan and Kaveh, 2013a).

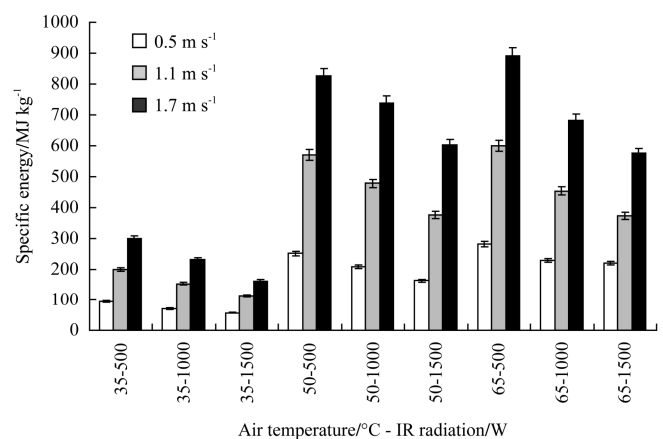


Figure 8 Specific energy consumption for thin layer drying of high moisture sour cherry at different levels of air temperatures, air velocities and IR radiations

Relationship between specific energy consumption and input parameters is as follow:

$$SEC = 474.19 + 180.7v - 74.94P + 165.59T_c + 81.72vT_c - 44.2vP - 164.4T_c^2$$

$$R^2=0.9737 \tag{22}$$

3.5 Neural network modeling

Tables 6 and 7 summarize a list of the best neural network topology structure, threshold functions and

different applied algorithms in predicting D_{eff} and SEC for drying of sour cherry. As shown in the mentioned tables, most applied topologies and threshold functions have proper training and validation errors. In fact, it could be asserted that the neural network is a powerful tool for

modeling of sour cherry drying in different conditions, which have a high accuracy and low cost and time. The main reason of neural network convergence might be the large amount of the network input patterns.

Table 6 Best selected topologies including training algorithm, different layers and neurons for D_{eff} predication

Network	Training algorithm	Threshold function	Number of layers and neurons	EMSE	R^2	MAE	SD_{MAE}	Epoch
FFBP	LM	TANSIG-LOGSIG-TANSIG	3-3-3-1	0.0141	0.9816	2.73×10^{-11}	2.38×10^{-11}	8
		TANSIG	3-2-3-1	0.0001	0.9944	2.23×10^{-11}	1.98×10^{-11}	27
	BR	LOGSIG-PURELIN-TANSIG	3-4-3-1	0.0633	0.9762	4.63×10^{-11}	4.28×10^{-11}	14
		TANSIG	3-2-3-1	0.0715	0.9651	4.72×10^{-11}	4.27×10^{-11}	14
CFBP	LM	TANSIG-LOGSIG-TANSIG	3-3-3-1	0.0060	0.9705	7.28×10^{-11}	6.93×10^{-11}	8
		TANSIG	3-3-3-1	0.0037	0.9802	3.22×10^{-11}	2.77×10^{-11}	7
	BR	TANSIG-PURELIN-TANSIG	3-4-3-1	0.0055	0.9779	3.69×10^{-11}	3.21×10^{-11}	10
		TANSIG	3-2-3-1	0.0037	0.9807	3.57×10^{-11}	3.17×10^{-11}	19

Table 7 Best selected topologies including training algorithm, different layers and neurons for specific energy consumption predication

Network	Training algorithm	Threshold function	Number of layers and neurons	EMSE	R^2	MAE	SD_{MAE}	Epoch
FFBP	LM	TANSIG-LOGSIG-TANSIG	3-2-3-1	0.0022	0.9782	34.72	8.7	14
		LOGSIG-PURELIN-TANSIG	3-4-3-1	0.0031	0.9701	57.11	12.9	11
	BR	TANSIG	3-3-3-1	0.0028	0.9750	35.04	10.3	26
		TANSIG	3-2-3-1	0.0097	0.9620	84.03	17.6	27
CFBP	LM	TANSIG-LOGSIG-TANSIG	3-3-3-1	0.0001	0.9905	25.10	6.8	8
		TANSIG-PURELIN-TANSIG	3-2-3-1	0.0010	0.9739	56.80	10.7	13

Two strategies of similar and various threshold functions for all layers were utilized to study effect of different threshold functions on FFBP and CFBP outputs (Tables 6 and 7). Both strategies, as well as learning algorithms of LM and BR, were used for training of FFBP and CFBP networks. Several topologies were selected as the best results from each network, training algorithm and threshold functions.

The best results for FFBP neural network for D_{eff} (Table 6) belonged to 3-2-3-1 topology and TANSIG threshold function with LM algorithm in the first strategy. This structure generated $RMSE=0.0001$, $R^2=0.9944$ and $MAE=2.23 \times 10^{-11}$ converged in 27 epochs.

The best results for FFBP neural network for specific energy consumption (Table 7) belonged to 3-2-3-1 topology and TANSIG-LOGSIG-TANSIG threshold function with LM algorithm in the first strategy. This

structure generated $RMSE=0.0022$, $R^2=0.9782$ and $MAE=34.72$ converged in 14 epochs.

The best results for CFBP neural network for D_{eff} belonged to topology of 3-2-3-1 with BR algorithm, threshold function of TANSIG and the first strategy. This composition output was $MAE=3.57 \times 10^{-11}$ and $R^2=0.9807$ at 19 training epochs. Also, the best results for CFBP network for specific energy consumption belonged to topology of 3-3-3-1 with BR algorithm, threshold function of TANSIG-LOGSIG-TANSIG and the first strategy. This composition output was $MAE=25.10$ and $R^2=0.9905$ at eight training epochs.

Figure 9 compares the predicted values with the desired output values on a plot of moisture diffusivity and energy consumption for infrared drying of sour cherry using the optimal static ANN.

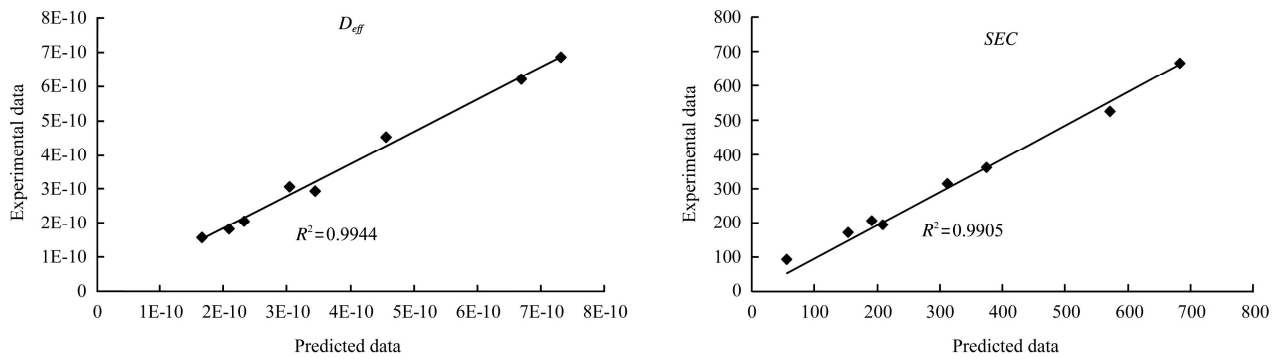


Figure 9 Predicted values of effective moisture diffusivity (D_{eff}) and specific energy consumption (SEC) using artificial neural networks versus experimental values for testing data set

This indicates the fact that the obtained ANN model can assuredly replace the mathematically constitutive models for infrared dryer parameters prediction, since it takes acceptable performance into account experimental data and automatically improves itself through learning. In addition, the ANN models have the ability to relearn to improve their performance if new data are available. This means that the optimum ANN model has the ability to improve prediction performance with new experiments. This topology can be used as a unique powerful model in automatic control system.

Figure 9 showed the data points are banded around a 45° straight line, demonstrating the suitability of the selected static multilayer feed-forward ANNs in predicting the kinetics analysis of infrared drying of sour cherry fruit. Process control and simulation in drying technology has always been a quite challenging task due to the non-linearity of drying phenomena and time-varying properties. Therefore, the ANN method is an attractive alternative to common approaches, which can give a higher accuracy and make it possible to estimate in a wider range.

4 Conclusions

Sour cherry fruit drying behavior in a laboratory infrared dryer with air drying temperatures of 35, 50 and 65°C, air velocity of 0.5, 1.1 and 1.7 m/s and IR radiation of 500, 1,000 and 1,500 W were studied. Drying air

temperature, air velocity and IR radiation, were important factors in drying time. The effective moisture diffusivity, activation energy and specific energy consumption of sour cherry were computed. The results showed that the best model for predicting drying kinetic was the Midilli et al. The effective moisture diffusivity values ranged from 1.17×10^{-10} to 8.13×10^{-10} m²/s. The highest effective moisture diffusivity derived at air velocity of 1.1 m/s, temperature of 65°C and IR radiation of 1,500 W. The activation energy (E_a) values ranged from 30.31 to 41.68 kJ/mol. The specific energy consumption values ranged from 56.12 to 891.16 MJ/kg. A multilayer feed and cascade forward artificial neural network (ANN) trained by back propagation algorithms was developed to predict the moisture diffusivity and energy consumption based on the three input variables. The ANN model with 3-2-3-1 and 3-3-3-1 topologies with the training algorithm of trainlm and threshold functions of tansig and tansig-logsig-tansig, respectively, were the best for predicting of moisture diffusivity and specific energy consumption of sour cherry fruit under infrared drying condition. This MLP topology was capable of learning the relationship between input parameters (air temperature, air velocity and IR radiation) and output parameter (moisture diffusivity and specific energy consumption) for studied infrared drying as indicated by low *RMSE* and *MAE*.

References

- Aghbashlo, M., M. H. Kianmehr, and S. R. Hassan-Beygi. 2010. Drying and rehydration characteristics of sour cherry (*Prunus cerasus* L.). *Journal of Food Processing and Preservation*, 34(3): 351-365.

- Aghbashlo, M., M. H. Kianmehr, and H. Samimi Akhijahani. 2008. Influence of drying conditions on the effective moisture diffusivity, energy of activation and energy consumption during the thin-layer drying of beriberi fruit (Berberidaceae). *Energy Conversion and Management*, 49(10): 2865-2871.
- Amiri Chayjan, R., and M. Kaveh. 2013a. Physical parameters and kinetic modeling of fix and fluid bed drying of terebinth seeds. *Journal of Food Processing and Preservation*, doi:10.1111/jfpp.12092. (in press)
- Amiri Chayjan, R., K. Salari, Q. Abedi, and A. A. Sabziparvar. 2013b. Modeling of moisture diffusivity, activation energy and specific energy consumption of squash seeds in a semi fluidized and fluidized bed drying. *Journal of Food Science and Technology*, DOI 10.1007/s13197-011-0399-8. (in press)
- Amiri Chayjan, R., J. Amiri Parian, and M. Esna-Ashari. 2011. Modeling of moisture diffusivity, activation energy and specific energy consumption of high moisture corn in a fixed and fluidized bed convective dryer. *Spanish Journal of Agricultural Research*, 9(1): 28-40.
- ASAE. 2007. ASAE Standard S352.2: moisture measurement- unground grain and seeds, 54th ed. ST Joseph, MI, USA.
- Basman, A., and S. Yalcin. 2011. Quick-boiling noodle production by using infrared drying. *Journal of Food Engineering*, 106(3): 245-252.
- Cakmak, G., and C. Yildiz. 2011. The prediction of seedy grape drying rate using a neural network method. *Computers and Electronics in Agriculture*, 75(1): 132-138.
- Cihan, A., K. Kahveci, and O. Hacıhafızoglu. 2007. Modeling of intermittent drying of thin layer rough rice. *Journal of Food Engineering*, 79(1): 293-298.
- Crank, J. 1975. Mathematics of diffusion (2nd ed.) London: Oxford University Press.
- Das, I., S. K. Das, and S. Bal. 2009. Drying kinetics of high moisture paddy undergoing vibration-assisted infrared (IR) drying. *Journal of Food Engineering*, 95(1): 166-171.
- Demir, V., T. Gunhan, and A. K. Yagcioglu. 2007. Mathematical modeling of convection drying of green table olives. *Biosystems Engineering*, 98(1): 47-53.
- Demuth, H., M. Beale, and M. Hagan. 2007. Neural network toolbox 5. The MathWorks, Natick, MA, USA.
- Dondee, S., N. Meeso, S. Soponronnarit, and S. Siriamornpun. 2011. Reducing cracking and breakage of soybean grains under combined near-infrared radiation and fluidized-bed drying. *Journal of Food Engineering*, 104(1): 6-13.
- Erenturk, S., and K. Erenturk. 2007. Comparison of genetic algorithm and neural network approaches for the drying process of carrot. *Journal of Food Engineering*, 78(3): 905-912.
- FAO. 2011. Statistical database. <http://www.faostat.fao.org/> (accessed 2013).
- Khair, R., Z. Pan, A. Salim, B. R. Hartsough, and S. Mohamed. 2011. Moisture diffusivity of rough rice under infrared radiation drying. *LWT - Food Science and Technology*, 44(4): 1126-1132.
- Khoshtaghaza, M. H., M. Sadeghi, and R. Amiri Chayjan. 2007. Study of rough rice drying process in fixed and fluidized bed conditions. *Journal of Agriculture Science and Natural Resource*, 14(2): 127-137. (in Persian)
- Markowski, M., I. Białobrzewski, and A. Modrzewska. 2010. Kinetics of spouted-bed drying of barley: Diffusivities for sphere and ellipsoid. *Journal of Food Engineering*, 96(3): 380-387.
- Menlik, T., M. B. Ozdemir, and V. Kirmaci. 2010. Determination of freeze-drying behaviors of apples by artificial neural network. *Expert Systems with Applications*, 37: 7669-7677.
- Midilli, A., H. Kucuk, and Z. Yapar. 2002. A new model for single-layer drying. *Drying Technology*, 20(7): 1503-1513.
- Mohebbi, M., F. Shahidi, M. Fathi, A. Ehtiati, and M. Noshad. 2011. Prediction of moisture content in pre-osmosed and ultrasounded dried banana using genetic algorithm and neural network. *Food and Bioprocesses Processing*, 89(4): 362-366
- Motevali, A., S. Younji, R. Amiri Chayjan, N. Aghilinategh, and A. Banakar. 2013. Drying kinetics of dill leaves in a convective dryer. *International Agrophysics*, 27(1): 39-47.
- Niamnuy, C., M. Nachaisin, N. Poomsa-ad, and S. Devahastin. 2012. Kinetic modelling of drying and conversion/ degradation of isoflavones during infrared drying of soybean. *Food Chemistry*, 133(3): 946-952.
- Nimmol, C., S. Devahastin, T. Swasdisevi, and S. Soponronnarit. 2007. Drying and heat transfer behavior of banana undergoing combined low-pressure superheated steam and far-infrared radiation drying. *Applied Thermal Engineering*, 27(14-15): 2483-2494.
- Odjo, S., P. Malumba, J. Dossou, S. Janas, and F. Béra. 2012. Influence of drying and hydrothermal treatment of corn on the denaturation of salt-soluble proteins and color parameters. *Journal of Food Engineering*, 109(3): 561-570.
- Pahlavan, R., M. Omid, and A. Akram. 2012. Energy input - output analysis and application of artificial neural networks for predicting greenhouse basil production. *Energy*, 37(1): 171-176.
- Perea-Flores, M. J., V. Garibay-Febles, J. J. Chanona-Pérez, G. Calderón-Domínguez, J. V. Méndez-Méndez, E. Palacios-González, and G. F. Gutiérrez-López. 2012. Mathematical modelling of castor oil seeds (*Ricinus communis*) drying kinetics in fluidized bed at high temperatures. *Industrial Crops and Products*, 38: 64-71.
- Ponkham, K., N. Meeso, S. Soponronnarit, and S. Siriamornpun. 2011. Modeling of combined far-infrared radiation and air drying of a ring shaped-pineapple with/without shrinkage.

- Food and Bioproducts Processing*, 90(2): 155-164.
- Ruiz Celma, A., F. Cuadros, and F. López-Rodríguez. 2012. Convective drying characteristics of sludge from treatment plants in tomato processing industries. *Food and Bioproducts Processing*, 90(2): 224-234.
- Ruiz Celma, A., F. López-Rodríguez, and F. Cuadros Blázquez. 2009a. Experimental modelling of infrared drying of industrial grape by-products. *Food and Bioproducts Processing*, 87(4): 247-253.
- Ruiz Celma, A., F. Cuadros, and F. López-Rodríguez. 2009b. Characterisation of industrial tomato by-products from infrared drying process. *Food and Bioproducts Processing*, 87(4): 282-291.
- Sakai, N., and W. Mao. 2006. Infrared heating. In: Sun, D.-W. (Ed.), *Thermal Food Processing: New Technologies and Quality Issues*. CRC Press LLC, USA.
- Shafafi Zenoozian, M., and S. Devahastin. 2009. Application of wavelet transform coupled with artificial neural network for predicting physicochemical properties of osmotically dehydrated pumpkin. *Journal of Food Engineering*, 90(2): 219-227.
- Shen, F., L. Peng, Y. Zhang, J. Wu, X. Zhang, G. Yang, H. Peng, H. Qi, and S.h. Deng. 2011. Thin-layer drying kinetics and quality changes of sweet sorghum stalk for ethanol production as affected by drying temperature. *Industrial Crops and Products*, 34(3): 1588-1594.
- Shi, J., Z. Pan, T. H. McHugh, D. Wood, E. Hirschberg, and D. Olson. 2008. Drying and quality characteristics of fresh and sugar-infused blueberries dried with infrared radiation heating. *LWT - Food Science and Technology*, 41(10): 1962-1972.
- Thuwapanichayanan, R., S. Prachayawarakorn, J. Kunwisawa, and S. Soponronnarit. 2011. Determination of effective moisture diffusivity and assessment of quality attributes of banana slices during drying. *LWT - Food Science and Technology*, 44(6): 1502-1510.
- Togrul, H. 2006. Suitable drying model for infrared drying of carrot. *Journal of Food Engineering*, 77(3): 610-619.
- Yadollahinia, A., and M. Jahangiri. 2009. Shrinkage of potato slices during drying. *Journal of Food Engineering*, 94(1): 52-58.
- Zhu, Y., Z. Pan, T. H. McHugh, and D. M. Barrett. 2010. Processing and quality characteristics of apple slices processed under simultaneous infrared dry-blanching and dehydration with intermittent heating. *Journal of Food Engineering*, 97(1): 8-16.
- Zielinska, M., and S. Cenkowski. 2012. Superheated steam drying characteristic and moisture diffusivity of distillers' wet grains and condensed distillers' solubles. *Journal of Food Engineering*, 109(3): 627-634.